

Axial Dispersion Study in Fixed Bed Columns

MARCELA POPA, IOAN MAMALIGA, **STELIAN PETRESCU**, EUGENIA TEODORA IACOB TUDOSE*

Technical University "Gheorghe Asachi" of Iasi, Faculty of Chemical Engineering and Environmental Protection, Chemical Engineering Department, 73 Dimitrie Mangeron Av., 700050, Iasi, Romania

Axial mixing in a fixed bed column, with porous cylindrical particles, has been studied. The experiments were conducted at atmospheric pressure, two different temperature values (30°C, 50°C) and several liquid (water) phase flowrates (7.65, 12.6, 17.5, 22.2 L/h). Granular cylindrical particles of charcoal as the solid phase and distilled water, as the liquid phase, have been used. The pulse response technique with a sodium chloride solution has been utilized. The distribution function of the residence times ($E(\theta)$), the Bodenstein number (Bo) and the axial dispersion coefficient (D_L) have been experimentally established. The obtained experimental data reveal the temperature and the liquid phase velocity (Reynolds number) effects on the Bodenstein number and the axial dispersion coefficient. Based on the mixing cell model, the cell number and the $E(\theta)$ function have been calculated, the last one being compared to the experimental distribution function $E(\theta)$.

Keywords: fixed bed, axial dispersion, mixing cell model

Fixed bed columns are often used in chemical engineering industry in physical operations (such as absorption, leaching, rectification) and in two- or three-phase chemical operations. Fluid flow in such equipment induces axial mixing (dispersion) which can be quantified using the axial dispersion coefficient. Besides the axial dispersion, radial liquid dispersion occurs, the latter one being however less intensive.

The axial dispersion is an important parameter affecting the performance of fixed bed columns, thus, the literature indicates a large number of theoretical and experimental studies on the subject [1-22].

Tsotsas and Schlünder [7] present a theoretical study related to the axial dispersion dependence on flow in fixed beds. They define three types of flow: micro-, meso- and macroscopic. In their study, the large discrepancy obtained for gas dispersion data is attributed to the mesoscopic flow which is described using a model. Also, the dependence of macroscopic flow and axial dispersion is discussed.

Jacksson and Harmon [8] established the axial dispersion coefficient in fixed beds for small Reynolds numbers ($Re < 0.1$). The dispersion coefficient values were determined experimentally in the form of $Pe = f(Re \cdot Sc)$ for methane dispersion in supercritical CO_2 .

A mathematical model was proposed for axial and radial dispersions in a porous cylindrical granular fixed bed by Arora and Kukreja [9]. The model was solved numerically via the finite element method using the orthogonal collocation technique. Crittenden, Brinkmann and Field [11] determined the axial dispersion coefficient in pulsed and non-pulsed liquid flow in a spherical particle fixed bed column.

Nigam, Iliuță and Larachi [14] have studied experimentally the axial dispersion in a gas-liquid cocurrent flow fixed bed column containing different shaped catalyst particles. They have determined experimentally the liquid Péclet number, for different velocity values of the two phases. Perin, Chaudourne, Jallut and Lieto [15] have studied theoretically and experimentally the axial dispersion in a gas-liquid counter-current flow fixed bed column. The obtained values for Pe_L and Pe_g are compared to the literature values.

Delgado [16] analyzed experimental data from literature to characterize dispersion in porous media for different dispersion regimes. He established equations to determine the axial and the radial dispersion coefficients based on a large number of his own experimental and literature data.

The majority of axial dispersion studies focus on fixed beds containing non-porous particles, at room temperature.

The present paper studies the axial mixing (dispersion) in a liquid flow column with a fixed bed of cylindrical charcoal particles. The residence time distribution and the axial dispersion coefficient (D_L) for different temperature and liquid phase flowrate values are established. The number of cells and the exit age distribution function $E(\theta)$ are established using the mixing cell model. The latter parameter is compared to the distribution function that was established experimentally. Also, the temperature and the Reynolds number influence on the Bodenstein number has been studied.

For one phase fluid flow in a fixed granular bed, the axial dispersion model is given by [2]:

$$\frac{\partial c}{\partial t} + u \frac{\partial c}{\partial z} - D_L \frac{\partial^2 c}{\partial z^2} = 0 \quad (1)$$

The initial and boundary conditions are:

$$t = 0, \quad 0 < z < L, \quad c = 0 \quad (2)$$

$$t = 0, \quad z = 0, \quad c_0 u = cu - D_L \frac{\partial c}{\partial z} \quad (3)$$

$$t > 0, \quad z = L, \quad \frac{\partial c}{\partial z} = 0 \quad (4)$$

Solving the above equation (1) with the specified conditions (2) and (4) gives the exit age distribution function $E(\theta)$. The $E(\theta)$ function variance is given by:

$$\sigma_\theta^2 = \frac{2}{Pe} - \frac{2}{Pe^2} (1 - e^{-Pe}) \quad (5)$$

If Péclet number (Pe) has large values, the equation (5) simplifies to:

$$\sigma_\theta^2 = \frac{2}{Pe} \quad (6)$$

Using the equations (5) and (6), one can establish the Péclet number.

* email: et_tudose@yahoo.com or etudose@ch.tuiasi.ro

The axial dispersion coefficient can be obtained using the definition of Péclet number (σ_0^2 is established experimentally).

The Bodenstein number defined as:

$$Bo = \frac{vd}{\varepsilon D_L} \quad (7)$$

is usually used for granular fixed bed columns. The Péclet and Bodenstein number dependence is given by:

$$Bo = Pe \frac{d}{L} \quad (8)$$

Experimental part

The experimental set-up, presented in figure 1, was used to determine the residence time distribution and the axial dispersion coefficient in a liquid flow column with a granular fixed bed. The experimental set-up includes a fixed bed column (1), a liquid reservoir (2), a flowmeter (3) to measure the liquid flowrate, a conductometer (4) with a probe (5) to determine the solution electric conductivity at the column exit, a vessel (6) to immerse the conductometer probe and two digital thermometers (7) and (8) to measure the liquid phase temperatures at the column entrance and exit, respectively. The column (1) made of thermo-resistant glass, with an inside diameter, D , of 0.036 m and a total height of 0.45 m, has an outside heat proof glass jacket (1a). The column base is equipped with a stainless steel sieve (1b) which sustains the fixed bed (1c) containing cylindrical charcoal particles ($d = 3.1$ mm, $l = 4$ mm). The charcoal particles were coated with paraffin such that the tracer diffusion in particle pores is not allowed. The pores were blocked with paraffin vapors.

The column top is covered with a rubber cap having three apertures for the liquid distributor (1d), the tube that connects to the exterior (1e) and the digital thermometer (7), respectively. The liquid phase column outlet (1g) and water column jacket inlet and outlet, (1h) and (1i), respectively, are also indicated in figure 1.

The experiments have been conducted at atmospheric pressure, two temperatures (30 and 50°C) and different liquid flowrates (distilled water: 7.65, 13.3, 17.55 and 22.45 L/h).

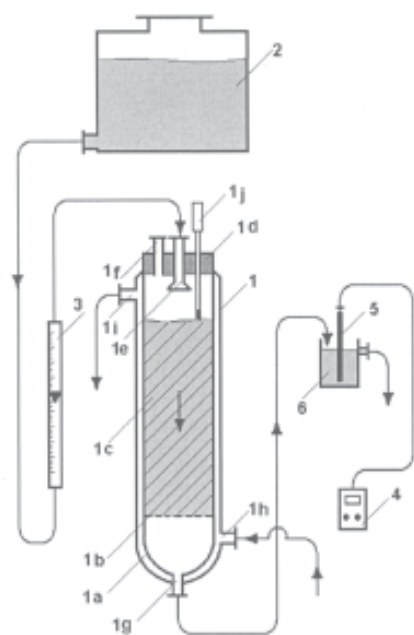


Fig. 1. Experimental setup (1 - fixed bed column, 2 - liquid reservoir, 3 - flowmeter, 4 - conductometer, 5 - conductometer probe, 6 - vessel, 7, 8 - digital thermometers)

Results and discussions

The pulse response technique has been used to obtain experimentally the exit age distribution function. For this purpose, the tracer used has been a sodium chloride solution of 20% mass concentration. The tracer was introduced in a pulsed signal with a 20 mL capacity syringe. In each experiment, 5 mL solution was introduced at the column upper part and the timer was immediately started. Every five seconds, the liquid electric conductivity at the column exit was read with the conductometer (4). Table 1 presents experimental data for electric conductivity. Based on the calibration curve, previously obtained, the sodium chloride concentrations at the column exit were interpolated.

These results and the equations (9) and (10) have been used to render the average residence time value (t mean time) and the distribution function of the residence times $E(\theta)$ [2, 5]:

$$\bar{t} = \frac{\sum c_i t_i}{\sum c_i} \quad (9) \quad E(\theta) = \frac{c_i \bar{t}}{\sum c_i \Delta t_i} \quad (10)$$

In figures 4 and 5 the distribution functions of the residence times are graphically represented for different temperature and liquid flowrate values, indicating that the distribution functions $E(\theta)$ present a maximum in the neighborhood of $\theta = 1$ value.

For most of the dependencies, the maximum of the distribution function for the residence times corresponds to a value of $\theta < 1$, fact that reveals the existence of some preferential flow regions inside the granular fixed bed column. The preferential flow areas and the other flow "defects" determine the appearance of axial dispersion.

To establish the density function variance of the distribution $E(\theta)$, the following relation is used:

$$\sigma_0^2 = \frac{\sum c_i t_i^2}{\bar{t}^2 \sum c_i} - 1 \quad (11)$$

Next, based on the equations (5) and (6) and the dispersion function values $E(\theta)$, the Péclet number was determined and, finally, using the equation (8), the Bodenstein number was calculated. Because the charcoal particles have a cylindrical form, the particle diameter (d) was calculated as the product of the equivalent particle diameter (d_e) and the form factor (ψ).

Using the Bodenstein number definition (7), the axial dispersion coefficient (D_L) was determined. Figures 6 and 7 show graphically the Bodenstein number variation depending on the liquid phase fictitious speed (v) and the Reynolds number at temperatures of 30 and 50°C.

Figures 8 and 9 support the fact that the axial dispersion coefficient depends on the liquid phase velocity and the Reynolds number, at the same above mentioned temperature values.

As can be seen from figures 6 and 7, the Bodenstein number decreases with the liquid phase velocity and respectively, with the Reynolds number. For small values of the velocity and the Reynolds number, respectively, $Bo = f(v)$ and $Bo = f(Re)$ dependencies are practically linear. As for $Bo = f(v)$ dependencies, the temperature increase induces a decrease in the Bodenstein number. The temperature increase in $Bo = f(Re)$ dependencies generates an increase in the Bodenstein number. The temperature increase determines a decrease of the liquid phase dynamic viscosity and, consequently, an increase of the Reynolds number value.

Table 1
ELECTRIC CONDUCTIVITY OF NaCl SOLUTION AT THE COLUMN EXIT IN TIME

T (°C)	30°C				50°C				
	M (L/h)	7.65	13.3	17.55	22.45	7.65	13.3	17.55	22.45
t(s)									
0	0	0	0	0	0	0	0	0	0
5	0.1529	0.1567	0.1424	0.142	0.1544	0.1542	0.1391	0.273	
10	0.1527	0.1538	0.142	0.1416	0.1541	0.153	0.139	0.208	
15	0.1526	0.1524	0.1418	0.1421	0.1537	0.1521	0.1388	0.185	
20	0.1525	0.1508	0.1432	0.938	0.1534	0.1513	0.28	2.58	
25	0.1519	0.1515	1.027	10.75	0.1523	0.1546	6.02	16.77	
30	0.1512	2.68	8.98	16.5	0.1516	0.751	16.47	13.76	
35	0.1506	2.24	16.14	12.21	0.1507	4.49	17.39	8.21	
40	0.1539	5.55	15.05	7.12	0.1553	12.35	11.53	4.62	
45	0.222	14.86	11.11	3.97	0.239	15.77	7.6	2.5	
50	1.003	16.17	8	2.23	0.884	15.21	4.57	1.7	
55	3.72	15.35	4.63	1.375	2.6	12.28	2.71	1.016	
60	8.3	12.23	3.46	0.936	5.75	9.65	1.954	0.684	
65	12.24	8.48	1.99	0.644	9.66	6.38	1.15	0.549	
70	15.61	5.69	1.381	0.521	12.76	4.72	0.81	0.438	
75	16.54	3.88	0.952	0.409	14.83	3.18	0.662	0.356	
80	16.89	2.84	0.749	0.357	15.38	2.54	0.539	0.313	
85	13.84	2.41	0.607	0.32	14.86	1.894	0.472	0.285	
90	11.43	1.564	0.538	0.288	13.42	1.54	0.399	0.261	
95	9.12	1.216	0.46	0.263	11.18	1.099	0.357	0.246	
100	7.28	0.988	0.391	0.25	9.66	0.893	0.333	0.229	
105	6.1	0.816	0.355	0.234	7.81	0.759	0.314	0.218	
110	4.99	0.743	0.322	0.226	6.11	0.677	0.292	0.212	
115	3.84	0.636	0.297	0.215	4.62	0.574	0.268	0.206	
120	3.22	0.578	0.28	0.209	4.09	0.523	0.255	0.199	
125	2.48	0.519	0.267	0.201	3.45	0.476	0.243	0.194	
130	2.13	0.454	0.249	0.196	2.77	0.433	0.233	0.19	
135	1.848	0.423	0.239	0.193	2.31	0.405	0.224	0.186	
140	1.612	0.398	0.228	0.189	1.976	0.374	0.218	0.182	
145	1.423	0.375	0.22	0.185	1.774	0.355	0.211	0.179	
150	1.285	0.35	0.213	0.183	1.558	0.338	0.206	0.176	
155	1.142	0.328	0.208	0.181	1.345	0.324	0.202	0.174	
160	1.076	0.309	0.204	0.178	1.081	0.31	0.198	0.171	
165	0.988	0.301	0.199	0.175	1.026	0.295	0.196	0.169	
170	0.896	0.289	0.196	0.173	0.949	0.283	0.192	0.168	
175	0.839	0.28	0.192	0.171	0.861	0.272	0.188	0.167	
180	0.79	0.269	0.189	0.171	0.793	0.258	0.185	0.165	

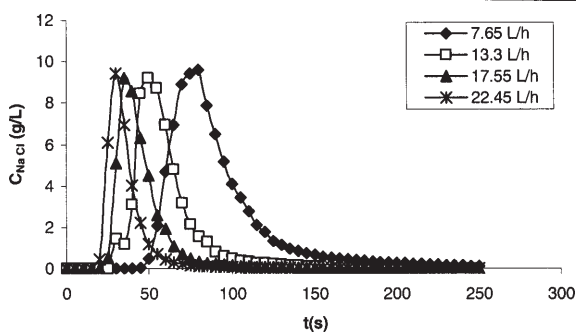


Fig. 2. Sodium chloride concentration variation in liquid phase, at the column exit as a function of time, T = 30°C

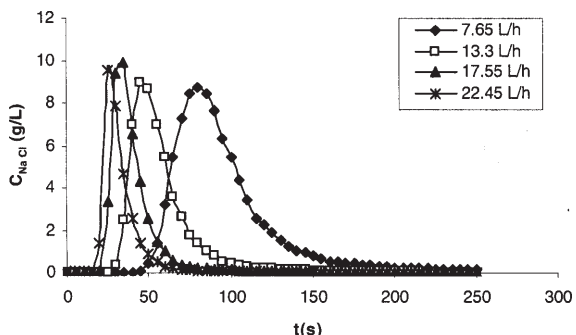


Fig. 3. Sodium chloride concentration variation in liquid phase, at the column exit as a function of time, T = 50°C

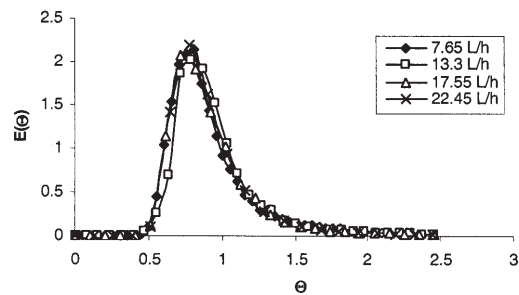


Fig. 4. The distribution functions of the residence times $E(\theta) = f(\theta)$, T = 30°C

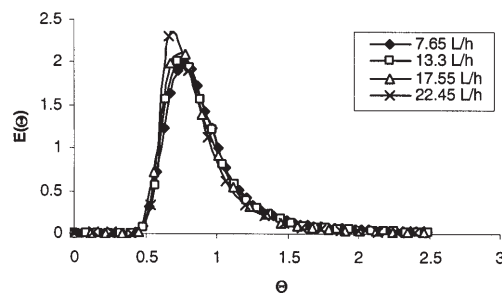


Fig. 5. The distribution functions of the residence times $E(\theta) = f(\theta)$, T = 50°C

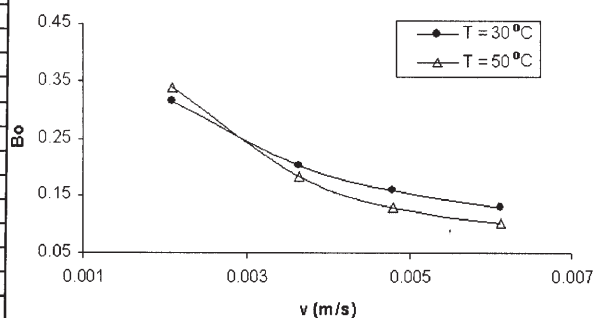


Fig. 6. Bodenstein number vs. liquid phase velocity at T = 30°C and respectively, 50°C

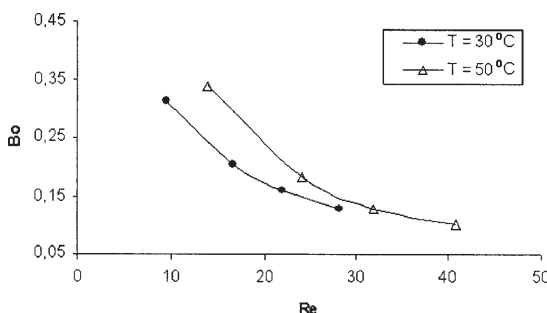


Fig. 7. Bodenstein number vs. Reynolds number at T = 30°C and respectively, 50°C

The diagram represented in figure 8 emphasizes an increase of the axial dispersion coefficient with the liquid phase velocity. This observation is also underlined in other studies [3, 11]. For small values of the liquid phase velocity, the increase of the axial dispersion coefficient D_L is negligible. As one can see from figure 8, the temperature influences positively the dispersion coefficient D_L , meaning that as the temperature value increases, so the coefficient D_L value does. This result is confirmed by other literature data [1].

Next, based on the mixing cell model, the cell number and the residence time distribution function were calculated. According to this model, the cell number and

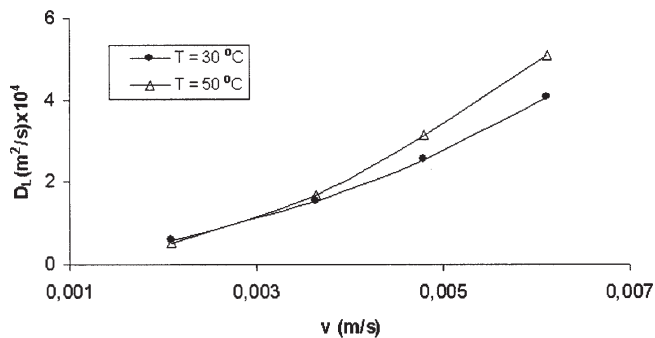


Fig. 8. The axial dispersion coefficient dependence on the liquid phase velocity at $T = 30^\circ\text{C}$ and respectively, 50°C

$v(\text{m/s})$	0.00479	0.00833	0.01100	0.01417
$T(^\circ\text{C})$				
30	12.66	8.19	6.45	5.20
50	13.69	7.42	5.22	4.13

Table 2
CELL NUMBER (n)

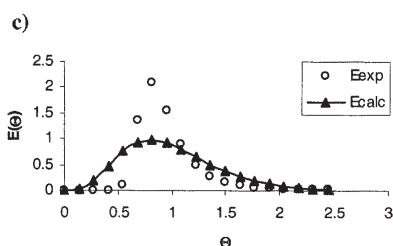
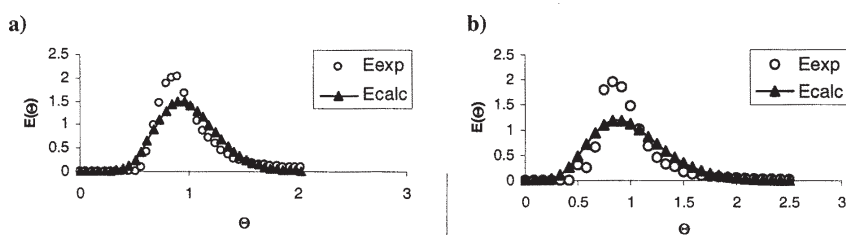


Fig. 9. Comparison between the dispersion functions $E(\theta)_{\text{exp}} = f(\theta)$ and $E(\theta)_{\text{calc}} = f(\theta)$, $T = 30^\circ\text{C}$: a) $M_v = 7.65 \text{ L/h}$, b) $M_v = 13.3 \text{ L/h}$, c) $M_v = 22.45 \text{ L/h}$

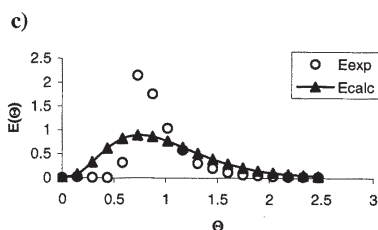
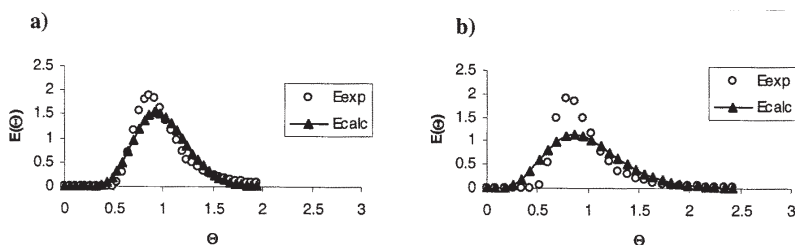


Fig. 10. Comparison between the dispersion functions $E(\theta)_{\text{exp}} = f(\theta)$ and $E(\theta) = f(\theta)$, $T = 50^\circ\text{C}$: a) $M_v = 7.65 \text{ L/h}$, b) $M_v = 13.3 \text{ L/h}$, c) $M_v = 22.45 \text{ L/h}$

the distribution function $E(\theta)$ are calculated using the following relations: (12)

$$n = \frac{1}{\sigma_\theta^2} \quad (13)$$

$$E(\theta) = \frac{n^n \theta^{n-1}}{(n-1)!} e^{-n\theta}$$

Using the experimental data for the distribution variance σ_θ^2 , the cell number has been determined. The obtained results are shown in the table 2.

Using equation (13) and table 2 data, the function values $E(\theta)$ were calculated and graphically represented in the figures 9 and 10.

The experimental determined values of $E(\theta)$ function are shown in the same graphs. Thus, it can be inferred that for small values of the liquid phase flowrate, up to 7.65 L/h , the values of the two functions $E(\theta)$, i.e. the $E(\theta)$ experimentally determined, $E(\theta)_{\text{exp}}$, and the $E(\theta)$ calculated based on the mixing cell model, $E(\theta)_{\text{calc}}$, are in good agreement. For larger values of the liquid flowrate, the two functions, $E(\theta)_{\text{exp}}$ and $E(\theta)_{\text{calc}}$ values are different.

This fact can be explained as follows: the fixed bed column used in this study has regions with preferential flow due to a ratio of column diameter to particle diameter D/d close to 10. When the liquid flowrate increases, the preferential flow intensifies and the axial dispersion

increases. Accordingly, the cell number is smaller, fact that will determine smaller $E(\theta)_{\text{calc}}$ values with respect to the $E(\theta)_{\text{exp}}$ values.

Conclusions

In this paper, axial mixing for a liquid phase flow in a fixed bed column, with porous cylindrical particles, has been studied.

Using a fixed bed column with charcoal cylindrical particles and distilled water as liquid phase, the distribution function of the residence times, $E(\theta)_{\text{exp}}$, and the distribution dispersion σ_{θ}^2 , for two different temperature values (30, 50°C) and different liquid flowrates, were experimentally determined.

Also, the Péclet and the Bodenstein numbers and the axial dispersion coefficient (D_L) were established via experiments.

Based on the mixing cell model, the cell number and the distribution function $E(\theta)_{\text{calc}}$ were determined. A good agreement between the two distribution functions, $E(\theta)_{\text{exp}}$ and $E(\theta)_{\text{calc}}$ is obtained only for small values of the liquid phase flowrate.

The experimental data within this study outline the temperature and the liquid phase velocity influences on the Bodenstein number and the axial dispersion coefficient.

Notations

c_0 - tracer concentration at the initial time, kg/m^3

c - tracer concentration at a certain time, kg/m^3

d - particle diameter, m

u - interstitial liquid velocity (in the intergranular space), m/s

v - liquid superficial velocity, m/s

D - column diameter, m

D_L - axial dispersion coefficient, m^2/s

L - fixed bed length (height), m

t - time, s

z - axial direction, m

c_c - tracer concentration at the column exit, at the initial time t_i , kg/m^3

\bar{t} - average residence time, s

$E(\theta)$ - distribution function of the residence times, dimensionless

$\Delta t_i (=t_i - t_{i-1})$ the time period between two consecutive electric conductivity readings, s

Pe - the Péclet number ($Pe = uL/D_L$), dimensionless

Bo - the Bodenstein number ($Bo = vd/\varepsilon D_L$), dimensionless

Re - the Reynolds number ($Re = \rho vd/\eta$), dimensionless

ε - the fixed bed porosity, dimensionless

ρ - the liquid density, kg/m^3

η - the liquid dynamic viscosity, Pa·s

σ_{θ}^2 - the $E(\theta)$ function dispersion, dimensionless

n - the cell number, dimensionless

θ - dimensionless time ($\theta = t/\bar{t}$), dimensionless

References

1. KAFAROV, V., Fundamentals of Mass Transfer, Mir Publishers, Moscow, 1975.
2. BOZGA, G., MUNTEAN, O., Reactoare chimice, vol.1. Reactoare omogene, Ed. Tehnică, București, 2000.
3. RICHARDSON, J.F., PEACOCK, D.G., Chemical Engineering, Vol.3, Prentice Hall, London, 1994.
4. DUTKAI, E., Coloane cu umplutură în tehnologia chimică, Ed. Tehnică, București, 1977.
5. COULSON, J.M., RICHARDSON, J.F., Chemical Engineering, Vol.2, Butterworth-Heinemann, Oxford, 1997.
6. PETRESCU, S., MĂMĂLIGĂ, I., CURTEANU, S., DIACONESCU, R., Reactoare chimice pentru reactoare omogene, Ed. Matrix Rom, București, 2001.
7. TSOTSAS, E., SCHLÜNDER, E.U., Chem. Eng. Process, **24**, nr. 1, 1988, p.15.
8. JACKSON, D.Y.K., HARMON, T.C., Chem. Eng. Science, **54**, nr. 3, 1999, p. 357.
9. ARORA, S., DHALIWAL, S.S., KUKREJA, V.K., Computers and Chemical Engineering, **30**, 2006, p.1054.
10. BURDETT, I.D., WEBB, D.R., DAVIS, G.A., Chem. Eng. Sci., **36**, nr. 12, 1981, p.1915.
11. CRITTENDEN, B.D., LAU, BRINKMANN, A., T., R.W. Field, Chem. Eng. Sci., **60**, 2005, p.111.
12. SOLCOVA, O., SOUKUP, K., SCHNEIDER, P., Chem. Eng. J., **110**, 2005, p.11.
13. MIYAUCHI, T., KIKUCHI, T., Chem. Eng. Sci., **30**, nr. 3, 1975, p.343.
14. NIGHAM, K.D.P., ILIUȚĂ, I., LARACHI, F., Chem. Eng. Process, **41**, 2002, p.365.
15. PERRIN, S., CHAUDOURNE, S., JALLUT, C., LIETO, J., Chem. Eng. Sci., **57**, 2002, p.3335.
16. DELGADO, J.M.P.Q., Chem. Eng. Res. Design, **85**, nr. 19, 2007, p.1245.
17. GUEDES DE CARVALHO, J.R.F., DELGADO, J.M.P.Q., Chem. Eng. Sci., **60**, 2005, p.365.
18. GHOREISHI, S.M., AKGERMAN, A., Sep. Purif. Techn., **39**, 2004, p.39.
19. CHO, Y.J., YANG, H.C., EUN, H.C., YOO, J.H., KIM, J.H., Chem. Eng. Process, **44**, 2005, p.1054.
20. HAMDAN, E., MILTHORPE, J.F., LAI, J.C.S., Chem. Eng. J., **137**, 2008, p.614.
21. HOROBA, C. A., MAMALIGA, I., Rev. Chim. (Bucharest), **65**, no. 8, 2014, p.907.
22. POPA, M., ONUTU, I., Rev. Chim. (Bucharest), **61**, no. 1, 2010, p.94.

Manuscript received: 15.09.2014